

Supplementary Material

Synthesis, Characterization and Anticancer Properties of an Oxovanadium(IV)-Sunitinib Complex

Germán López Robledo,^a Lucía Santa María de la Parra,^b Khalil Jori,^c Gonzalo Scalese,^d José Martín Ramallo López,^c Boris Emilio Rodenak-Kladniew^e, Ignacio Esteban León^{*b,f} and María Soledad Islas^{*a}

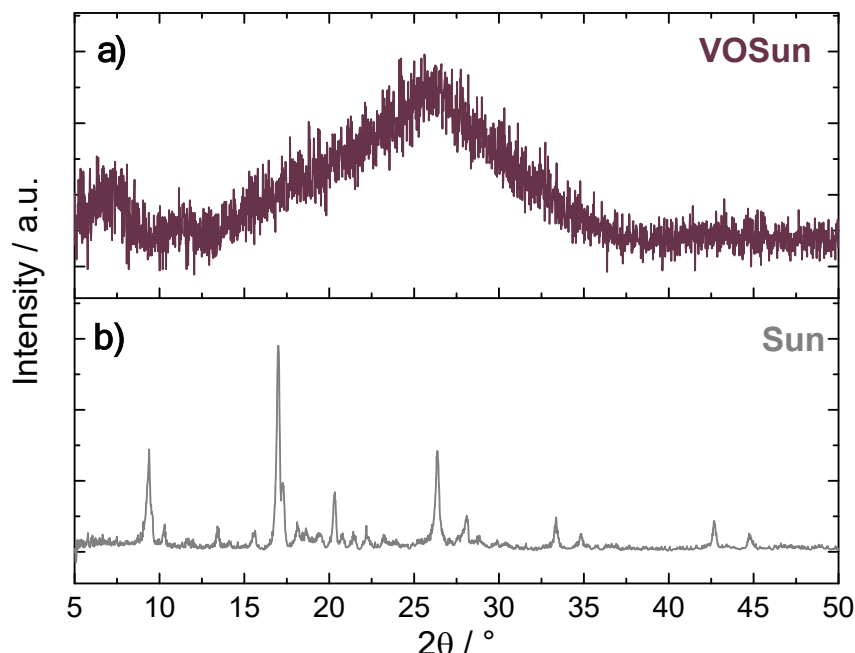


Figure S1. XRD pattern of sunitinib (Sun, gray), and vanadium(IV) complex (VOSun, in dark red).

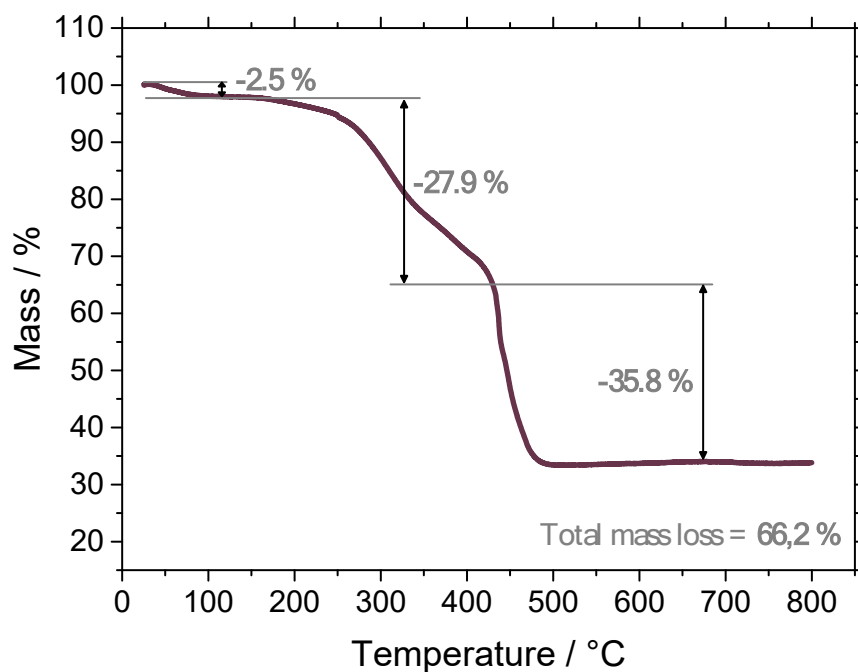


Figure S2. Thermogravimetric analysis (TGA) for VOSun. Weight losses are marked in %.

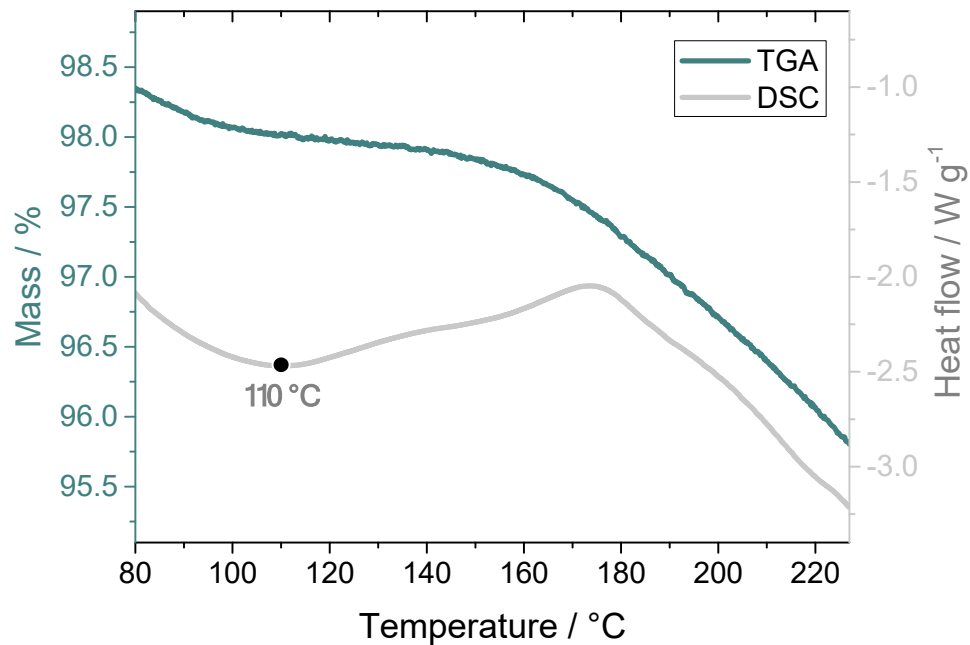


Figure S3. Differential Scanning Calorimetry (DSC, in gray) and TGA (in green) for VOSun. Broad endothermic peak at 110 °C is shown.

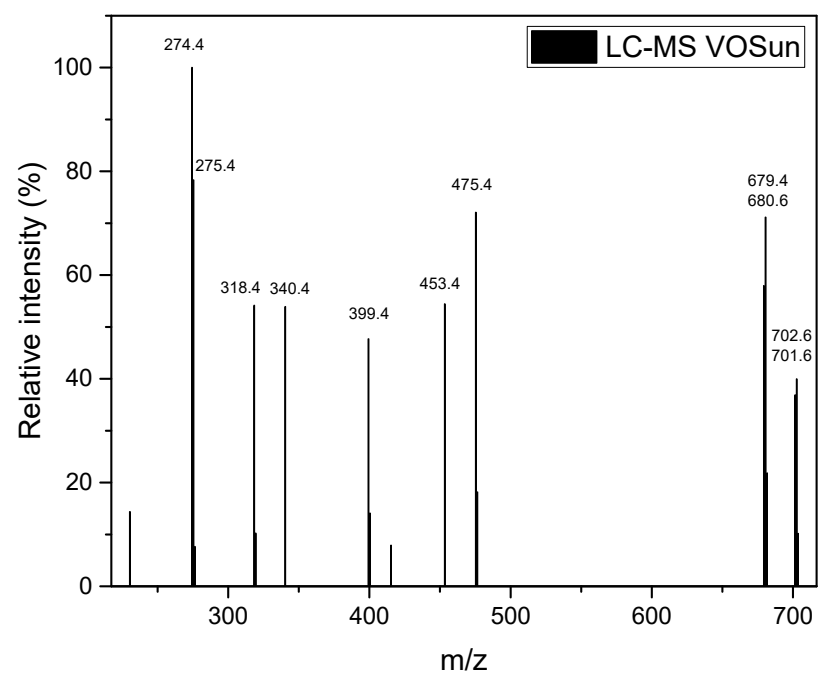


Figure S4. LC- single MS spectrum of VOSun (5 ppm) in acetonitrile.

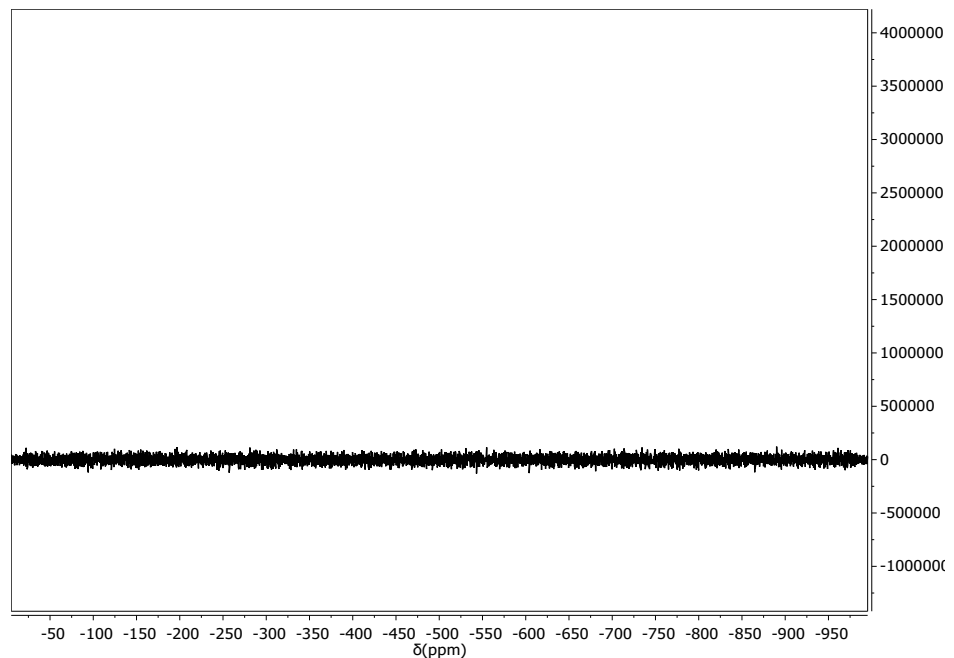


Figure S5. ^{51}V NMR of 2.1 mM VOSun in $\text{DMSO}-d_6$ immediately after dissolution

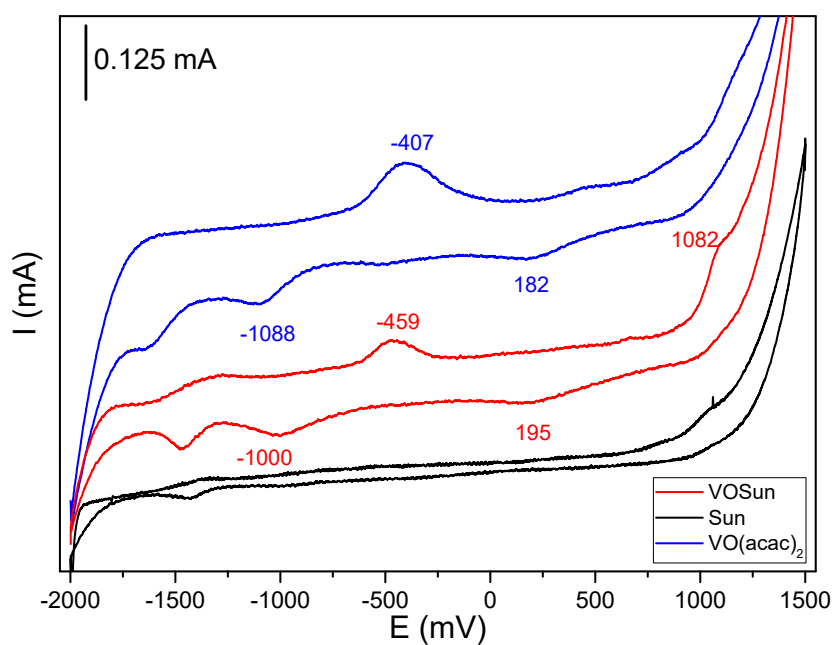


Figure S6. Cyclic voltammetry (vs. Ag./AgCl) of Sun in its basic form (black), the VOSun complex (red), and $\text{VO}(\text{acac})_2$ (blue). All at a concentration of 0.001 M in DMSO, using TBAPF_6 0.1 M as the supporting electrolyte, preceded by nitrogen bubbling. $v=100$ mV/s. The graph highlights the main identified peaks (in mV).

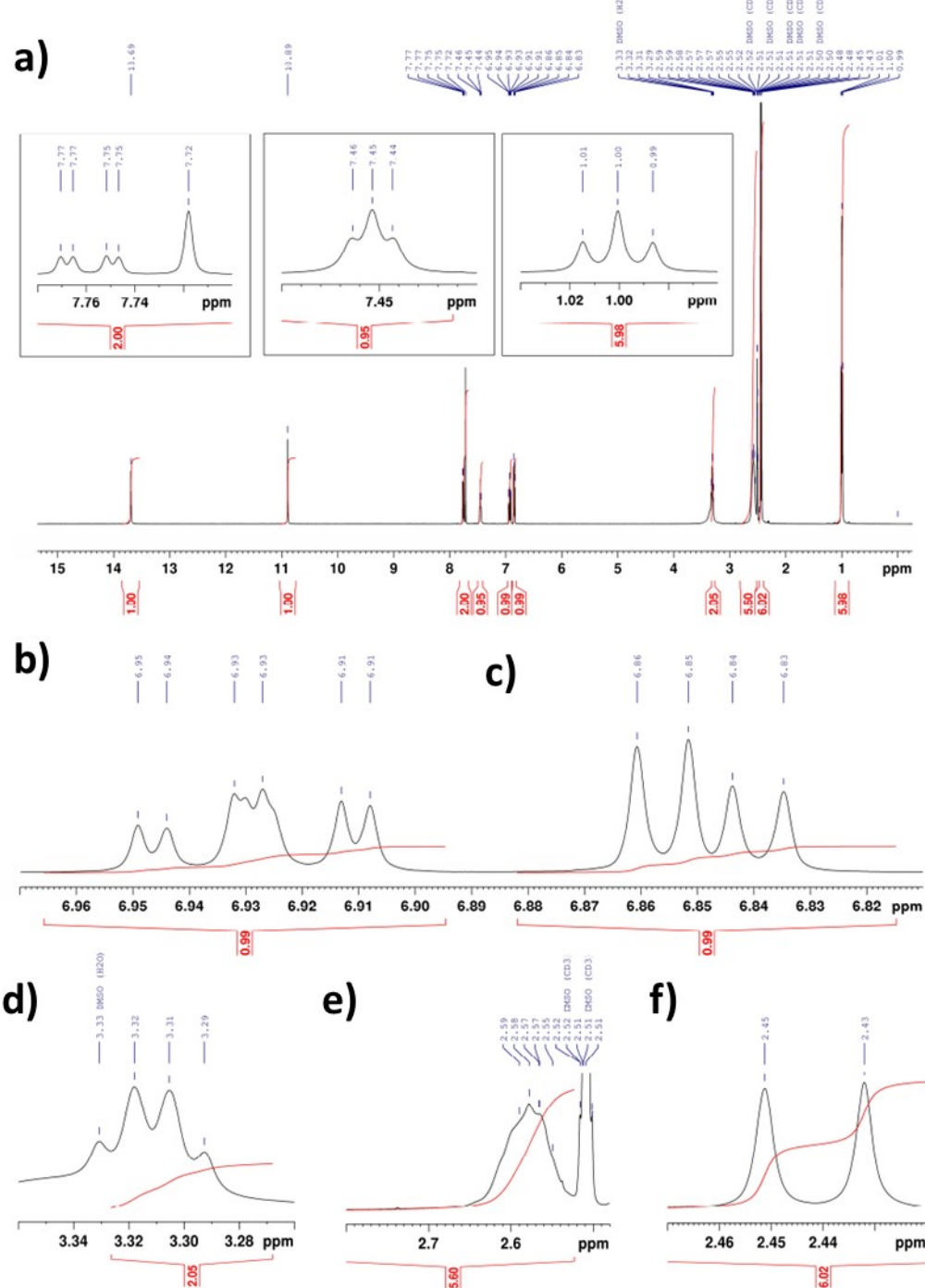


Figure S7. Sunitinib ^1H -NMR (500 MHz) spectrum in DMSO-d_6 solution. In blue: chemical shifts (solvent impurities are also shown in blue), in red: integration area for each peak. a) Full ^1H -NMR spectrum. b-f) magnification of different regions. b) H-7; c) H-8; d) H-9; e) H-10, H-11 and H-12; f) H-13 and H-14.

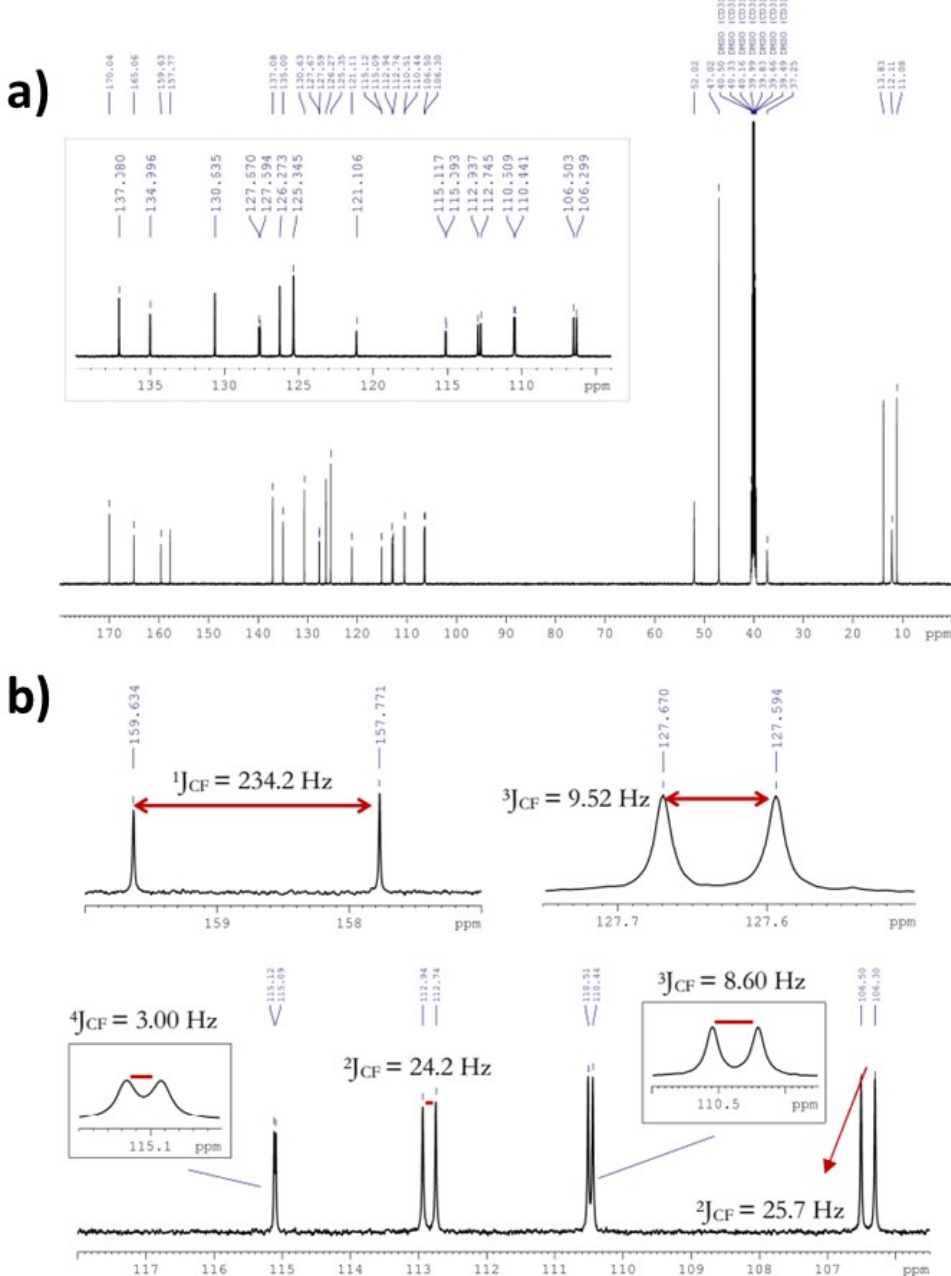


Figure S8. Sunitinib ^{13}C -NMR (125 MHz) spectrum in DMSO- d_6 solution. a) Chemical shifts and solvent impurities are shown in blue. Inset: magnification of the 140–100 ppm region. b) Magnification with $^1\text{J}_{\text{CF}}$ coupling constant (in MHz) for each signal.

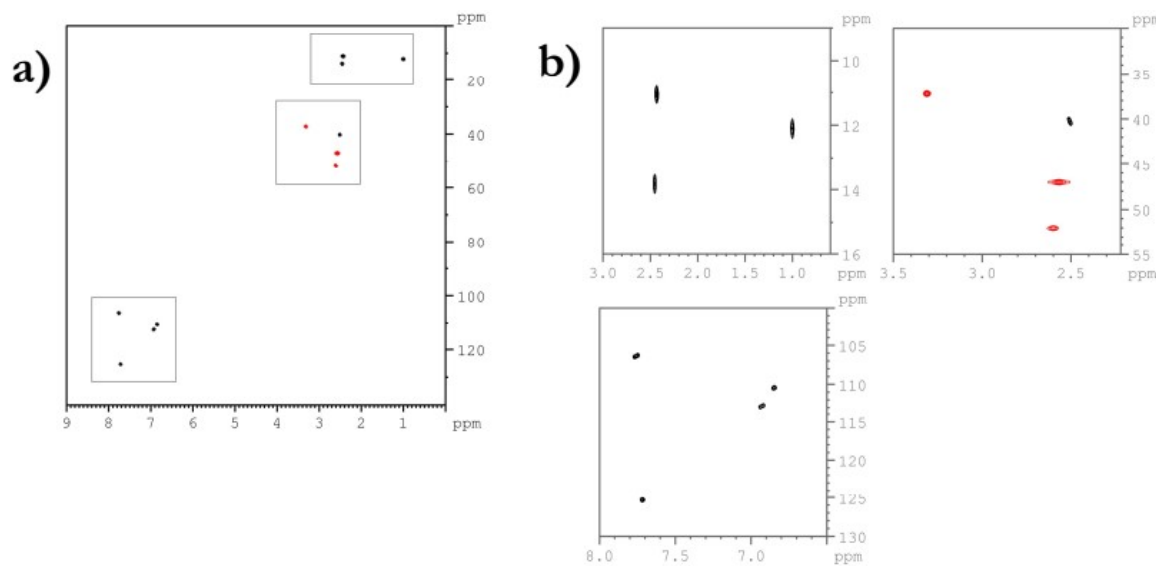


Figure S9. Sunitinib ^1H - ^{13}C HSQC spectrum (^1H : 500 MHz; ^{13}C : 125 MHz) in DMSO- d_6 solution. a) full spectrum, b) magnifications. In black: positive sign ($-\text{CH}-/\text{-CH}_3$); in red: negative sign ($-\text{CH}_2-$).

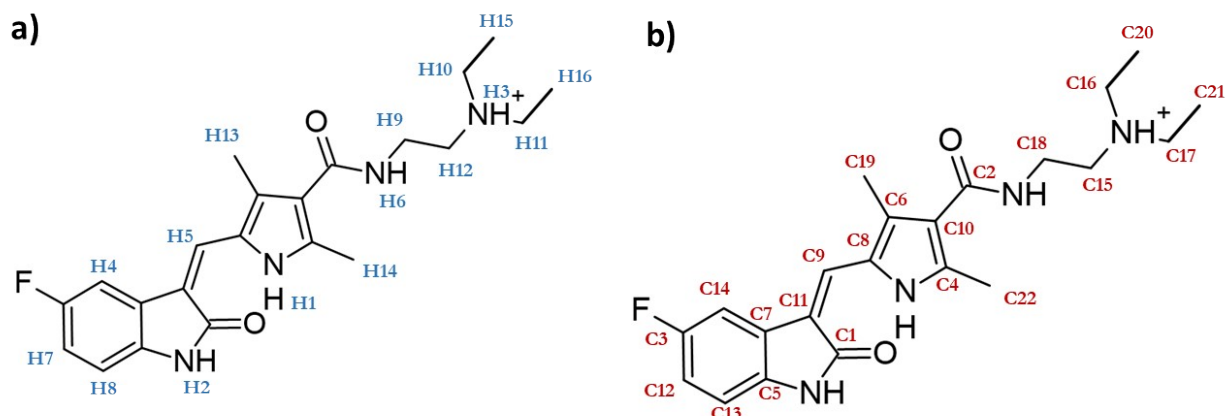


Figure S10. Atom numbering for a) proton (H) and b) carbon (C) used in table S1, Fig. 1, 2 and S10. In basic Sun $^1\text{H-NMR}$, no H-3 is present.

Table S1. Comparison and assignment for ^1H -NMR signals, splittings and areas. Correlation between ^1H and ^{13}C according to HSQC spectrum.

Assigmentation	$\delta(\text{H})$ Sun / ppm		$\delta(\text{H})$ VO Sun / ppm		$\delta(\text{H})$ Sun H^+ / ppm		Corr. HSQC (exp)
	Obs. (500 MHz)	Ref ¹ . (400 MHz)	Obs.	Ref ¹ . (400 MHz)	Ref ² . (400 MHz)	Ref ³ . (500 MHz)	
H-1 (-N-H)	13.69 (s, 1H)	13.69 (s, 1H)	13.75 (s, 1H)	13.75 (s, 1H)	13.74 (s, 1H)	13.73 (s, 1H)	-
H-2 (-N-H)	10.89 (s, 1H)	10.90 (s, 1H)	10.92 (s, 1H)	10.94 (s, 1H)	10.92 (s, 1H)	10.93 (s, 1H)	-
H-3 (-N ⁺ -H)	-	-	9.28 (br, 1H)	a	9.84 (br, 1H)	a	-
H-4 (-C-H)	7.76 (dd, 1H)	7.78 -7.75 (m, 1H)	7.77 (m, 1H)	7.77 (m, 1H)	7.79 - 7.76 (m, 1H)	7.77 (d, 1H)	C-14
H-5 (-C=C-H)	7.72 (s, 1H)	7.72 (s, 1H)	7.73 (s, 1H)	7.75 (s, 1H)	7.73 (s, 1H)	7.73 (s, 1H)	C-9
H-6 (-N-H)	7.45 (m, 1H)	7.46 -7.43 (m, 1H)	7.85 (m, 1H)	7.79 (dd, 1H)	7.89 (m, 1H)	7.72 (d, 1H)	-
H-7 (-C-H)	6.95 -6.91 (td, 1H)	6.95 -6.90 (m, 1H)	6.95 – 6.92 (m, 1H)	6.95 – 6.92 (m, 1H)	6.97 – 6.91 (m, 1H)	6.93 (d, 1H)	C-12
H-8 (-C-H)	6.85 (dd, 1H)	6.86 -6.83 (m, 1H)	6.86 – 6.84 (m, 1H)	6.87 – 6.84 (m, 1H)	6.87 – 6.84 (m, 1H)	6.87 (d, 1H)	C-13
H-9 (-CH ₂ -)	3.31 -3.29 (m, 2H)	3.31 -3.26 (m, 2H)	3.61 (br, 2H)	3.54 (m, 2H)	3.60 – 3.52 (m, 2H)	3.48 (br, 2H)	C-18
H-10 (-CH ₂ -)	2.70 -2.52 (br, 6H)	2.57 -2.51 (m, 6H)	3.27 (br, 6H)	3.09 – 3.07 (m, 6H)	3.24 – 3.20 (m, 6H)	2.96 (s, 6H)	C-16 C-17 C-15
H-13 (-CH ₃)	2.45 (s, 3H)	2.44 (s, 3H)	2.48 (s, 3H)	2.48 (s, 3H)	2.48 (s, 3H)	2.51 (s, 3H)	C-19
H-14 (-CH ₃)	2.43 (s, 3H)	2.43 (s, 3H)	2.46 (s, 3H)	2.45 (s, 3H)	2.46 (s, 3H)	2.44 (s, 3H)	C-22
H-15 (-CH ₃)	1.01 -0.99 (t, 6H)	1.00 -0.96 (t, 6H)	1.25 (br, 6H)	1.19 (t, 6H)	1.27 – 1.23 (t, 6H)	1.14 (t, 6H)	C-20 C-21

^a Chemical shift not informed for this exchangeable H in Sun H^+ .

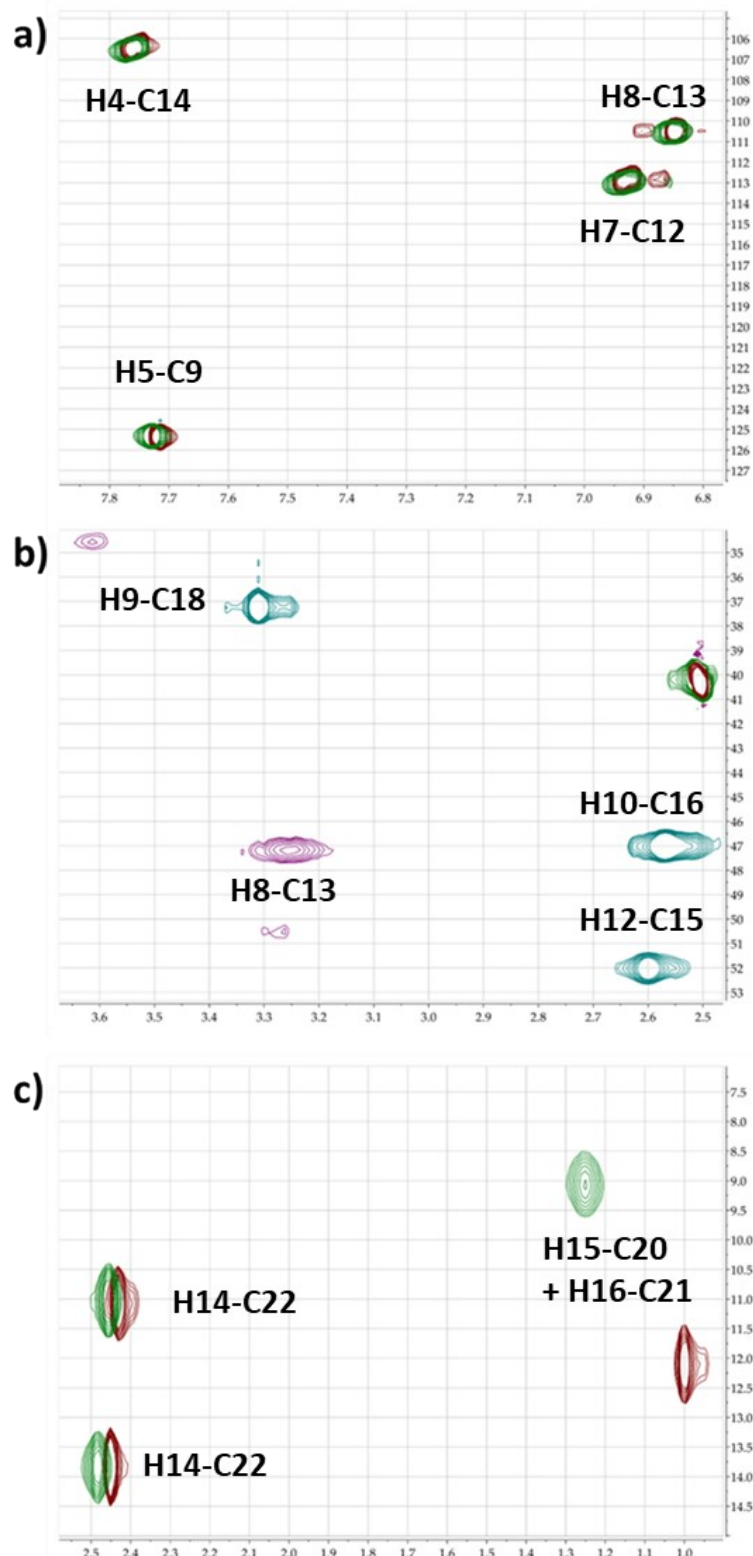


Figure S11. ^1H - ^{13}C HSQC of selected areas of Sun and VOSun. a) $\delta(\text{H}) = 7.8\text{-}6.8$, b) $\delta(\text{H}) = 3.6\text{-}2.5$, signal at $\delta(\text{C}) = 40$ is assigned to DMSO solvent, and c) $\delta(\text{H}) = 2.6\text{-}0.8$. For Sun: positive peaks are in green and negative in pink. For VOSun: positive peaks in red and negative peaks in blue. Hydrogen and carbon numbers are according to Fig. S9.

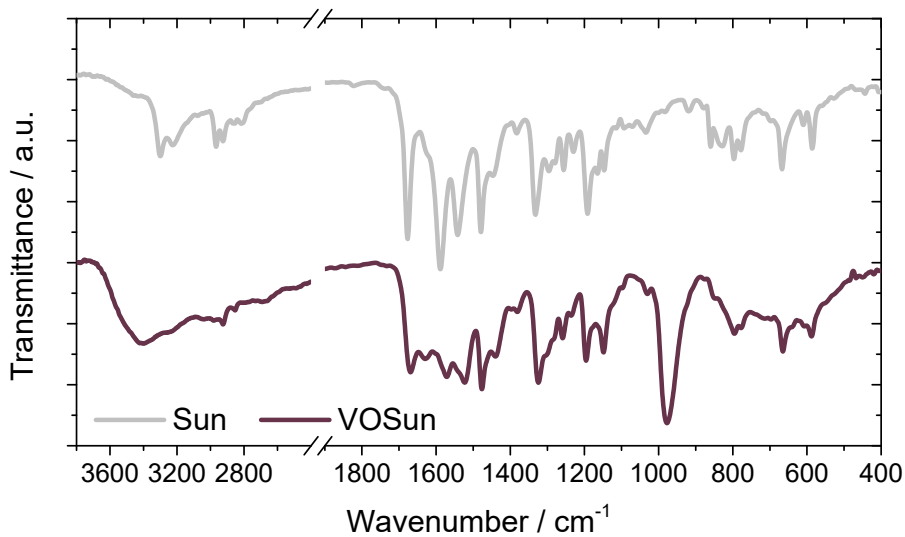


Figure S12. FTIR spectrum of Sun (gray) and VOSun (dark red).

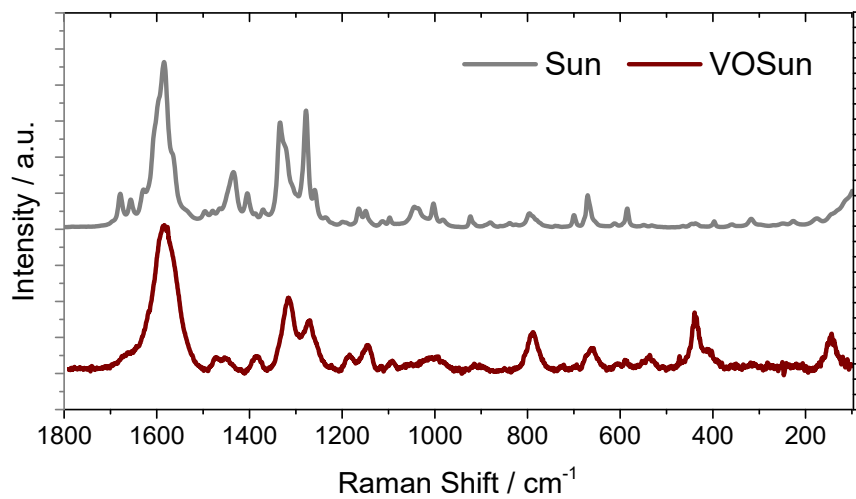


Figure S13. Raman spectrum of Sun (gray) and VOSun (dark red), in the region 1800 – 100 cm⁻¹.

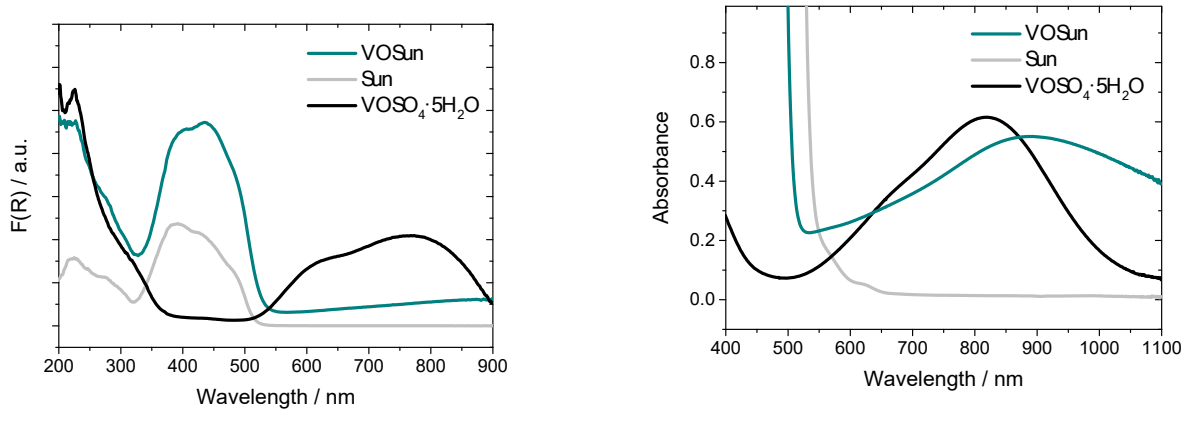


Figure S14. (a) UV-Vis diffuse reflectance spectra and (b) UV-Vis absorption spectra obtained in DMSO solution of VO(Sun) (light-blue), Sun (gray) and VOSO₄·5H₂O (black).

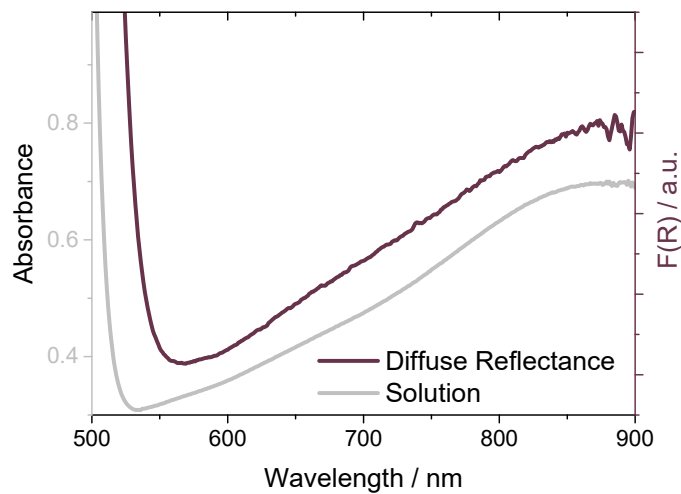


Figure S15. Comparison between UV-vis (in DMSO, in gray) and diffuse reflectance (dark red) spectra of VOSun.

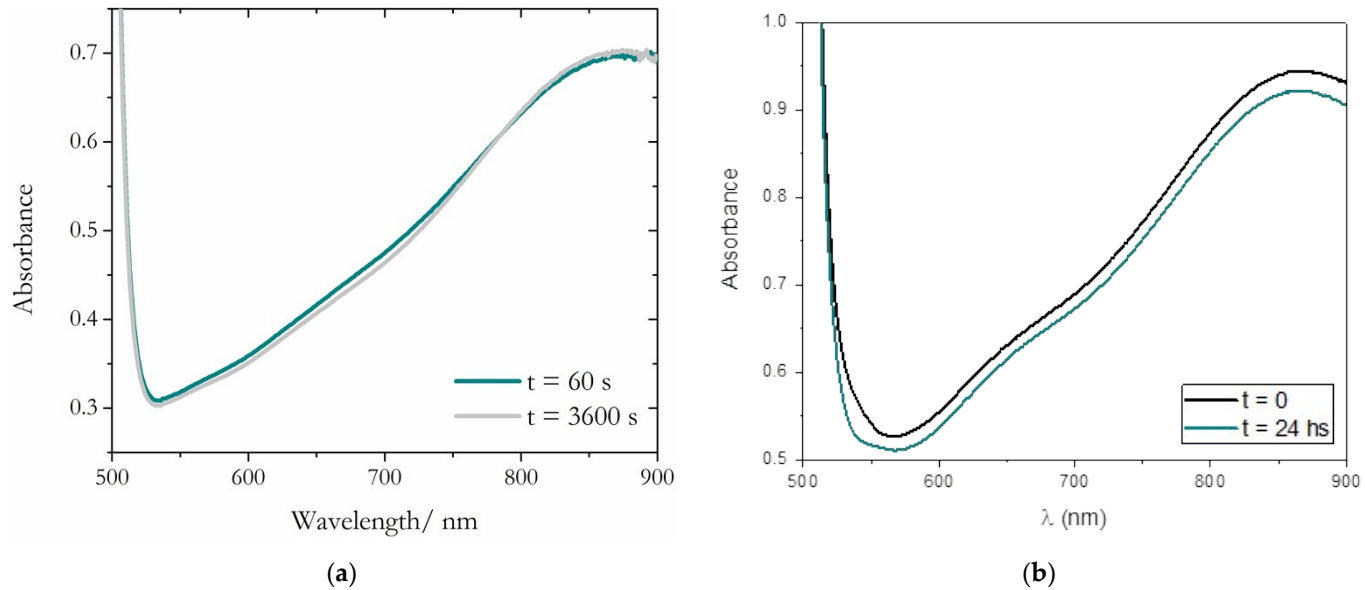


Figure S16. UV-vis spectra of VOSun in DMSO **(a)** at 60 and 3600 s (room temperature), **(b)** at 0 and 24 hs (37°C).

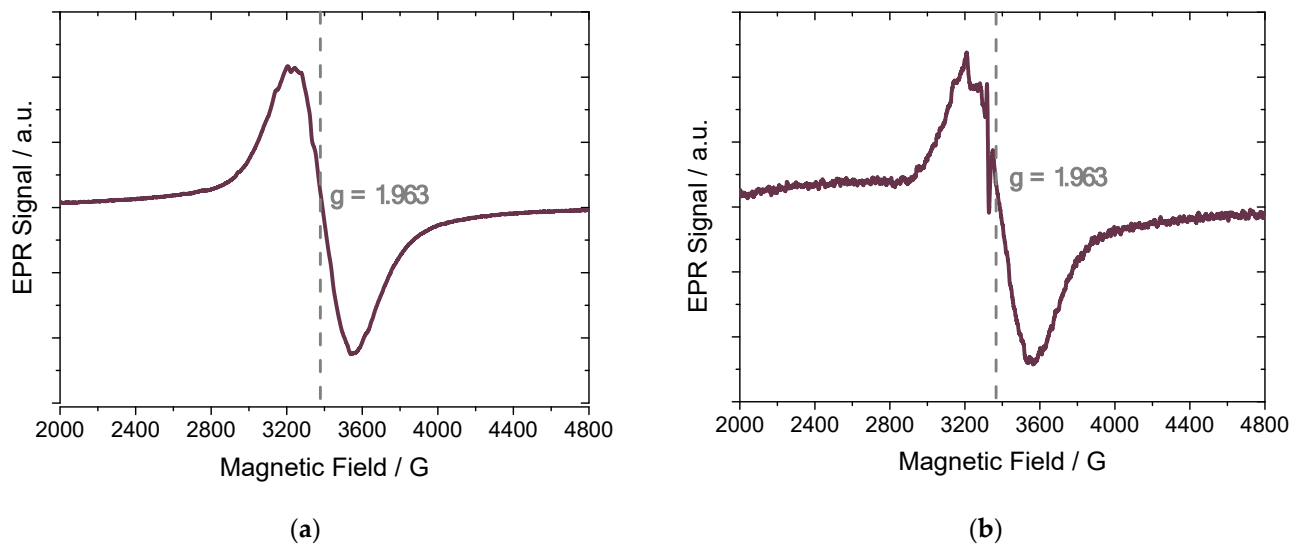


Figure S17. EPR spectra of complex VOSun measured in (a) solid phase ($T = 120\text{ K}$) and (b) DMSO solution ($T = 120\text{ K}$), in an X-band spectrometer.

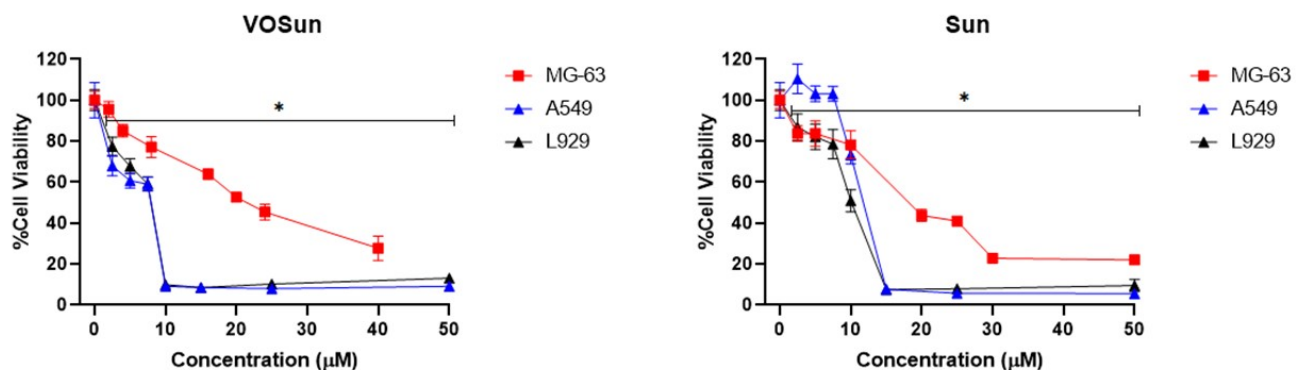


Figure S18. Cellular viability was evaluated via MTT assay. Cells were incubated in Dulbecco's modified Eagle's medium (DMEM) alone (control) or with different concentrations of compounds for 24 h. The results are expressed as the mean \pm the standard error of the mean (SEM). * $p < 0.0001$ differences between control and treatment.

- 1 G. Meng, C. Liu, S. Qin, M. Dong, X. Wei, M. Zheng, L. Qin, H. Wang, X. He and Z. Zhang, *Res. Chem. Intermed.*, 2015, **41**, 8941–8954.
- 2 F. Tarasi, P. A. Lanza, V. Ferretti, G. A. Echeverría, O. E. Piro, M. Cacicedo, S. Gehring, I. E. León and M. S. Islas, *Inorganics*, 2022, **10**, 1–16.
- 3 M. G. Kassem, A. F. M. Motiur Rahman and H. M. Korashy, 2012, pp. 363–388.